

A Numerical Analysis of the Tunnel-Diode Frequency Converter

M. R. BARBER, MEMBER, IEEE

Abstract—The theory of tunnel-diode mixer operation is briefly reviewed. It is shown how the available gain, minimum noise figure and output conductance can be expressed in terms of the bias and local oscillator voltages. A numerical analysis is then carried out for a large number of pairs of these voltages. The results show that there are two modes of low noise operation, both using approximately the same bias voltage which gives minimum noise when the diode is used as an amplifier. The minimum noise figure of one mode approaches that of the amplifier and is accompanied by very high gain, critical adjustment, and a vanishingly small local oscillator voltage. The more practical second mode on the other hand, uses a local oscillator power of about -7 dBm and gives a conversion loss lower than that obtainable from the best L-band varistor mixers, but with a slightly poorer noise figure.

The analysis could be applied equally well to optimize backward diode converters using megacycle intermediate frequencies in which only the second mode occurs.

INTRODUCTION

DURING THE past four years, numerous reports have appeared in the literature concerning the tunnel-diode frequency converter or mixer. Some authors have claimed noise figures lower than those obtained using the same diodes as amplifiers while others hold that the opposite is true. This paper intends to clarify the "mystery" surrounding this device and to demonstrate that the minimum noise figure of an ideal tunnel diode is the same whether it is used as an amplifier or as a frequency converter.

Chang, Heilmeier, and Prager [1] were probably the first to report practical results using a gallium-arsenide diode biased at a voltage slightly lower than the peak of the I-V characteristic. In the UHF range they claimed a noise figure of 2.8 dB, 1 dB lower than their calculated value. About the same time, Breitzer [2] claimed on the basis of calculation that the noise figure of the tunnel-diode mixer would generally be poorer than the amplifier. Peterson [3], a year later, pointed out approximations in Chang's analysis and confirmed Breitzer's calculations, although both Chang and Breitzer considered thermal noise generated in the load resistor in their noise figure derivations. Shih Fang Lo [4], on the other hand, discussed the advantages of ignoring load noise if the Friis cascade formula is to be used.

An extensive forty-page analysis of the tunnel-diode mixer has been published by Pucel [5] who concludes that the minimum noise figure should be obtained in the negative slope region. He has performed a numerical analysis to substantiate his claim. Sterzer and Presser [6] have also numerically analyzed a mixer and tested it

at 1340 Mc using a germanium tunnel diode. Although Sterzer apparently made no special attempt to optimize the source impedance, he reported a double sideband mixer-IF amplifier noise figure of 4.3 dB when operating at a bias voltage in the negative slope region and with a local oscillator power in excess of 0 dBm.

Dickens and Gneiting [7] claimed the noise figure of the mixer could possibly be lower than the amplifier when biased at the point of minimum IR product. Their lowest measured noise figure at 1200 Mc/s was 3 dB and occurred with very high conversion gain. Space limitations prevent further papers on this subject from being mentioned here; nevertheless, a considerable amount of work is being carried on and the literature is continuing to expand.

Pucel, Sterzer, Dickens and Breitzer appear to have been the only workers to stress the use of a bias point in the negative slope region. Only Pucel, however, mentions the possibility of using a very small pump power [5].

It will be shown here that there are two modes of low noise operation assuming a sinusoidal local oscillator voltage. Both modes use approximately the same bias voltage which gives minimum noise when the diode is used as an amplifier. With vanishingly small pump power the noise figure is seen to approach that of the amplifier, although, for this mode the mixer is extremely difficult to adjust as the exchangeable gain becomes very large. Using the same bias point but with a much larger pump power (-7 dBm approx.) a second, less critical, condition for moderately low noise figure is reached accompanied by a small conversion loss.

In the light of these results, it is now apparent that the previous workers have been divided between these two modes of operation. Pucel alone was aware that it might be possible to obtain good noise figures with vanishingly small pump powers. Dickens and Gneiting apparently discovered this mode by accident; they did not predict it theoretically. In the case of backward diode converters [8] the negative resistance region disappears and only the large pump mode exists.

MIXER GAIN AND IMPEDANCE FORMULAS

In what follows, it will be assumed that the tunnel-diode series inductance, series resistance, and time-varying junction capacitance can be neglected in the frequency range of interest, since their inclusion would unnecessarily complicate the analysis. In any case, an attempt is normally made either to tune out these parasitics or to incorporate them in the external circuitry.

Manuscript received April 21, 1965.

The author is with Bell Telephone Labs. Inc., Murray Hill, N. J.

The theory of crystal-diode mixer operation has been established for a number of years [9] and is directly applicable to the tunnel diode. By restricting the theory to power flow at the signal, image, local oscillator, and intermediate frequencies it is possible to represent the mixer by a three-port linear network, provided the local oscillator voltage is much greater than the signal voltage. Figure 1 shows a simplified three-port mixer in which currents at the signal, image, local oscillator, and intermediate frequencies can flow through the nonlinear conductance (G) but are otherwise separated by the filters F_α , F_γ , F_{l0} , and F_β . If the three-port mixer network is assumed to be reciprocal, an equivalent circuit can be drawn embodying the so-called conversion conductances as shown in Fig. 2, in which the voltages e_α , e_β , and e_γ are at the signal, IF, and image frequencies. The conversion conductances are the Fourier coefficients of conductance when the latter is time varying due to some arbitrary local oscillator voltage waveform applied across the diode:

$$g = g_0 + \sum_{n=1}^{\infty} 2g_{en} \cos n\omega_{l0}t. \quad (1)$$

An alternative equivalent, convenient for numerical analysis, is given in Fig. 3 in which signals at the three frequencies of interest have separate circuits. Note that neither Fig. 2 nor Fig. 3 utilize the conductances g_{e3} , g_{e4} , etc. which suggests either that conversion from frequencies near the higher local oscillator harmonics is neglected, or that these higher frequencies are short circuited. It will be assumed that the local oscillator frequency is not substantially lower than the signal frequency; otherwise it would be possible for the higher harmonics to lie in the region of the signal band where they could not be short circuited.

Using the circuits of Figs. 2 or 3 it is possible to establish the following equations that previously appeared in the literature in one form or another [4], [6]. The equations apply to the case where the image impedance is a short circuit, i.e., $g_\gamma = \infty$.

$$\text{Transducer gain} = \frac{4g_\alpha g_\beta g_{c1}^2}{[(g_0 + g_\beta)(g_0 + g_\alpha) - g_{c1}^2]^2}. \quad (2)$$

$$\text{Available gain} = \frac{g_\alpha}{g_{\text{out}}} \left(\frac{g_{c1}}{g_0 + g_\alpha} \right)^2. \quad (3)$$

$$\text{Output conductance } g_{\text{out}} = g_0 - \frac{g_{c1}^2}{g_0 + g_\alpha}. \quad (4)$$

$$\text{Input conductance } g_{\text{in}} = g_0 - \frac{g_{c1}^2}{g_0 + g_\beta} \quad (5)$$

where

g_α = source conductance.

g_β = load conductance.

In cases where the output conductance becomes negative, the available gain will be negative and referred to as the exchangeable power gain. This quantity can then

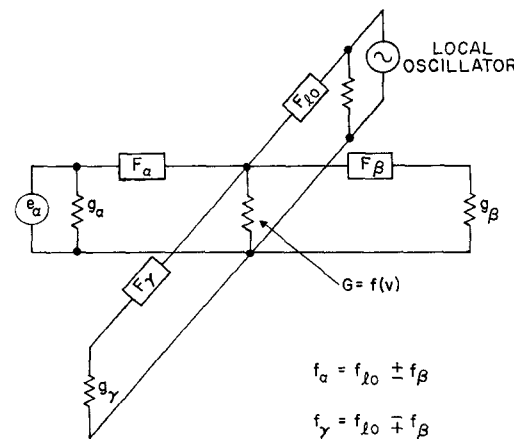


Fig. 1. Simplified mixer circuit.

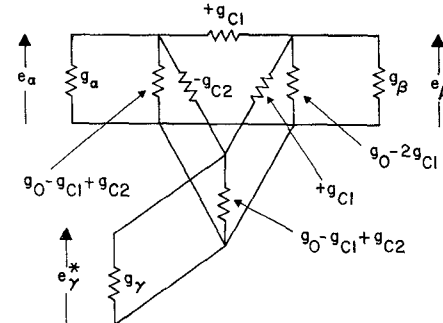


Fig. 2. Equivalent linear reciprocal network of a mixer diode.

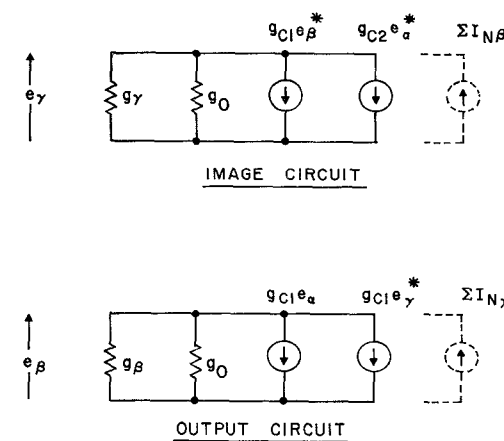
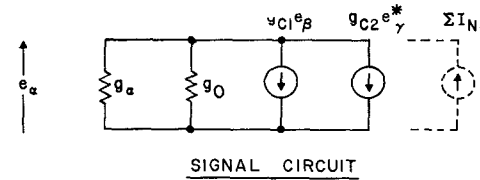


Fig. 3. Equivalent frequency-separated circuits of a shunt mixer diode.

be used directly in the Friis cascade noise formula if the mixer is followed by an IF amplifier. The proper value for the noise figure of the IF amplifier when connected to the negative output conductance of the mixer has been discussed by Haus and Adler [10].

The selection of sufficiently large source and load conductances to fulfill stability criteria will not be discussed here since this topic has been covered reasonably well in the literature [5], [11].

MIXER NOISE FORMULAS

The basic noise theory for crystal-diode mixers has been developed by Strutt [12]. He neglects thermal noise generated in the diode series resistance r_s and assumes that significant shot noise currents are generated with arbitrary phase which can be represented by the following set of fluctuation components:

$$\sqrt{2} I_{\text{rms}} \sum_{n=0}^{\infty} \{ \cos [(n\omega_{l0} + \omega_{\beta})t + a_n] + \cos [(n\omega_{l0} - \omega_{\beta})t + b_n] \} \quad (6)$$

where the coefficients n are integers. The rms current magnitude is determined by a well-known equation

$$I_{\text{rms}} = 2eI_{eq}\Delta f, \quad (7)$$

where I_{eq} is known as the equivalent shot-noise current and will be discussed in the next section. The essential feature of Strutt's analysis is that he assumes I_{eq} to be time-varying, due to the action of the local oscillator voltage, i.e.,

$$I_{eq} = I_{e0} + \sum_{n=1}^{\infty} 2I_{en} \cos n\omega_{l0}t. \quad (8)$$

If (7) and (8) are substituted into (6), a multitude of noise currents at different frequencies will appear, the most significant of which are illustrated in Fig. 3. In effect, noise originally generated at the intermediate frequency, for example, has been up-converted to the signal and image frequencies and vice versa. As a result of these conversion processes there is a definite phase relationship between the shot noise components at the signal, image, and intermediate frequencies when a local oscillator voltage is applied. The normal down-conversion process of the mixer, governed by (2), then acts to convert the various noise components to the intermediate frequency. It is not surprising, therefore, to find that correlation effects occur which often prove beneficial in lowering the noise figure.

Although shot noise currents are generated at frequencies near the higher harmonics of the local oscillator [see (6)], these are down-converted as a result of the amplitude modulation produced by local oscillator voltage. This process will occur even though voltages at these higher frequencies are short-circuited. Strutt's noise figure analysis will therefore apply when higher frequencies are shorted out.

Following Strutt with minor changes in notation, and

assuming that signals at the image frequency have been short-circuited, the following noise figure expression can be derived from Fig. 3, ignoring any noise generated in the load:

$$F = 1 + \frac{e}{2kT} \frac{1}{g_{\alpha}} \left[I_{e0} \left(\frac{g_0 + g_{\alpha}}{g_{c1}} \right)^2 + I_{e0} - 2I_{e1} \left(\frac{g_0 + g_{\alpha}}{g_{c1}} \right) \right] \quad (9)$$

where $g_{\gamma} = \infty$, g_{α} is the source conductance and g_0 , g_{c1} , I_{e0} , I_{e1} have been defined by (1) and (8). Of the three terms within the brackets, the first pertains to noise components down-converted from the signal frequency, the second to noise components existing at the intermediate frequency, and the final term to the interaction or correlation of signal and intermediate frequency noise.

For the case where $g_{\alpha} = g_{\gamma}$ we obtain the single-sideband noise figure which is generally 1 or 2 dB worse than for the case of a short-circuited image:

$$F_{\text{single sideband}} = 2 + \frac{e}{2kT} \frac{1}{g_{\alpha}} \left[I_{e0} \left(\frac{g_0 + g_{\alpha}}{g_{c1}} \right)^2 + 2I_{e0} + 2I_{e2} - 4I_{e1} \left(\frac{g_0 + g_{\alpha}}{g_{c1}} \right) \right]. \quad (10)$$

Apart from additional shot-noise effects, the main degradation of (10) compared to (9) has been caused by thermal noise in the image conductance. This accounts for the 2 at the left of the expression, assuming the image and signal conductances are at the same temperature.

Equation (9) has the minimum value

$$F_{\text{min}} = 1 + \frac{e}{kT} \frac{I_{e0}}{g_{c1}^2} \left[g_{\alpha_{\text{opt}}} + g_0 - g_{c1} \frac{I_{e1}}{I_{e0}} \right] \quad (11)$$

when

$$g_{\alpha}^2 = g_{\alpha_{\text{opt}}}^2 = g_0^2 - 2g_{c1}g_0 \frac{I_{e1}}{I_{e0}} + g_{c1}^2. \quad (12)$$

The right-hand side of (12) is always positive since $I_{eq} > 0$ at all times implying $|I_{e1}| \leq |I_{e0}|$. It is apparent from (11) that it is desirable to have a very small mean effective shot noise current I_{e0} . A low noise figure could also be achieved if the correlation term following the negative sign were to cancel $(g_{\alpha} + g_0)$. In practical cases however, cancellation does occur but is incomplete; typically $(g_{c1}I_{e1}/I_{e0}) = 0.4(g_{\alpha} + g_0)$ in the large pump mode which will be discussed later.

In the following computer analysis, use was made of (11) which assumes a short-circuited image. Although the double-sideband noise figure is the easiest to measure, the image short circuit result is the lowest which can be obtained in a single sideband system. The noise figure with short circuited image generally lies between the double- and single-channel noise figures.

Shot Noise in the Tunnel Diode

Assuming full shot noise, the mean-square value of current fluctuations in a semiconductor is

$$\overline{i^2} = 2eI_{eq}\Delta f. \quad (13)$$

It can be shown [13] for an idealized tunnel diode that I_{eq} is given by

$$I_{eq} = I_B \coth \left(\frac{eV}{2kT} \right), \quad (14)$$

where I_{eq} is the sum of two uncorrelated oppositely flowing current streams, namely, the tunneling and Zener breakdown currents. This quantity is plotted in Figs. 4 and 5 for typical germanium and gallium antimonide tunnel diodes.

Recent measurements by King and Sharpe [14] indicate that the idealized form of the I_{eq} vs. V characteristic often differs markedly from that found by actual measurement; examples are shown in Figs. 4 and 5. At zero bias voltage however, the noise current $I_{eq}(0)$ was found to agree in all cases with the theoretical value. It is of interest to note that thermodynamic considerations require the zero bias shot noise to be equal to the thermal noise produced by the dynamic conductance of the diode.

Generally I_{eq} is greater than the bias current I_B and this has the effect of raising the noise figure of tunnel-diode devices. In the following analysis use will be made of King and Sharpe's equivalent noise and bias current measurements [14]. In particular, mixer action will be calculated using the characteristics of Figs. 4 and 5 which were reproduced from [14]. Thermal noise will be neglected in the analysis although this contribution can be shown to be small well below the diode cutoff frequency. Flicker (1/f) noise will also be neglected, a reasonably valid assumption provided the intermediate frequency is of the order of 30 Mc/s.

NUMERICAL ANALYSIS OF ACTUAL DIODE CHARACTERISTICS

It is of interest to calculate minimum noise figure and available gain for the tunnel diode mixer and to compare the results with those obtainable using the same diode as a one-port amplifier. The three variables are the source conductance, the bias voltage and the amplitude of the local oscillator voltage. An assumption must be made concerning the LO voltage waveform but this will be predominantly sinusoidal if the source impedance is sufficiently low. Although a sinusoidal voltage generator may not be optimum for minimum noise, it is probably the most practical.

An analysis has been carried out for a range of bias and local oscillator voltages. At each pair of voltages the optimum source conductance, noise figure, available

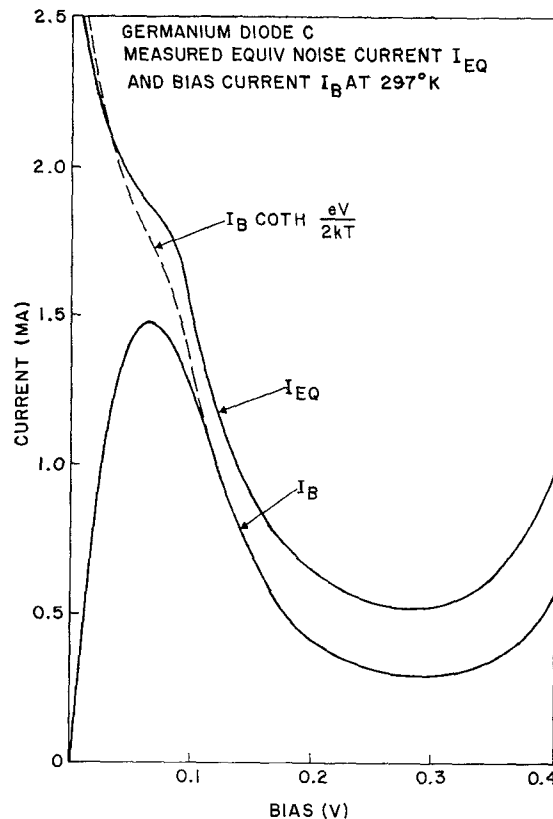


Fig. 4. Equivalent noise current and bias current for a Ge tunnel diode.

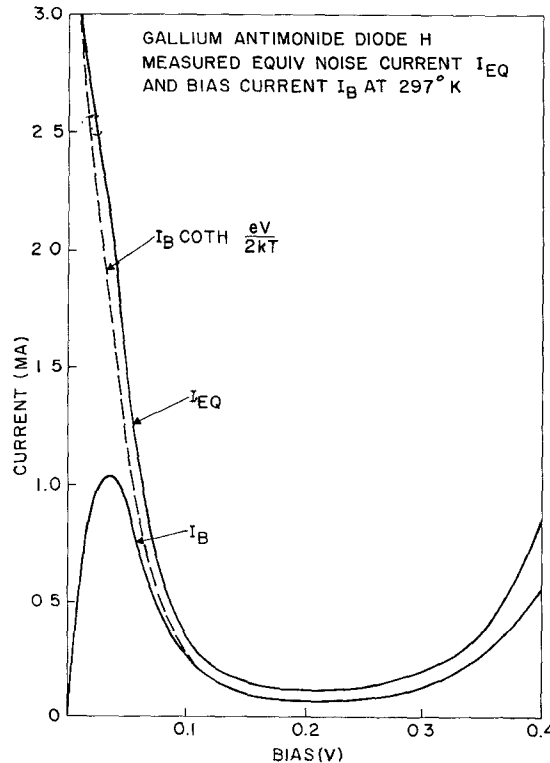


Fig. 5. Equivalent noise current and bias current for a GaSb tunnel diode.

gain, and output conductance were calculated using a procedure that will now be outlined.

Numerical Approximations

The first step in the mixer analysis is to determine a pair of functions that adequately describe the conductance and equivalent shot-noise characteristics in terms of applied voltage. One method is to use the Fourier series, another is to use exponentials, while a third is to use polynomials. If a sinusoidal local oscillator voltage is assumed it is possible to express V as

$$V = V_0 + V_{pk} \cos(\omega_{lo}t) \quad (15)$$

where V_0 is the dc bias voltage. Substitution of this expression in the appropriate function for g or I_{eq} then gives the conversion conductances g_0 , g_{c1} , g_{c2} , etc. If the Fourier series representation is used, g_0 , g_{c1} , etc. are obtained in terms of Bessel functions of the first kind; if the exponential approach is used the results appear in terms of modified Bessel functions while the polynomial approach gives them directly in terms of bias voltage (V_0) and peak local oscillator swing (V_{pk}).

Using a 10th-degree polynomial approximation through a prescribed set of 10 points it was found that large excursions occurred between the points. It was then decided that a Chebyshev approximation should be used which minimizes the extreme errors in contrast to a least-squares fit would have permitted an occasional large deviation. Polynomial regressions were therefore obtained using Chebyshev transforms which give $g(V)$ and $I_{eq}(V)$ in the form:

$$g, I_{eq} = \sum_{n=0}^n \alpha_n T_n(V) \quad (16)$$

where $T_n(V)$ is the n th-order Chebyshev polynomial. Figures 6 and 7 demonstrate the way in which typical 9th-degree polynomials agree with the original curves. In the case of the shot-noise characteristics (not shown) the fit was generally better than that of Fig. 7 due to the absence of any sharp curvature.

The polynomials were obtained using 40 data points spaced over extrapolated versions of King and Sharpe's original curves.

Calculation of Mixer Performance

The conversion conductances and shot-noise coefficients are obtained by substituting (15) into (16) and expressing the results in the form of (1) and (8). Substitution in (2)-(5) and (11) and (12) then yields such quantities as minimum noise factor, available gain, etc. The interpolated results of these calculations, carried out for 120 pairs of bias and local oscillator voltages, are given in Figs. 8 through 15. It is important to remember that in these figures the source conductance has been optimized at all points.

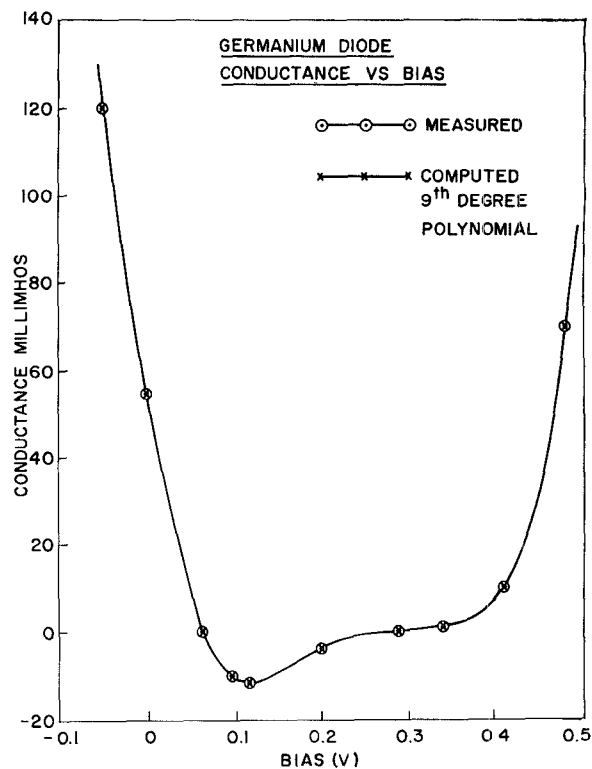


Fig. 6. Measured and computed conductances for the Ge diode characteristics of Fig. 4.

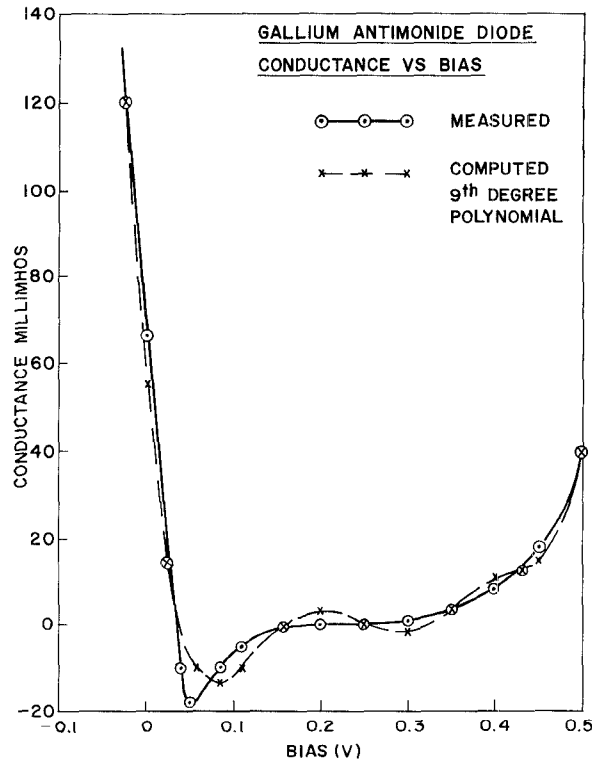


Fig. 7. Measured and computed conductances for the GaSb diode characteristics of Fig. 5.

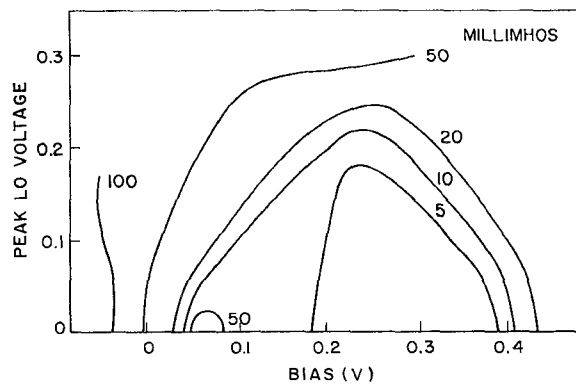


Fig. 8. Ge diode optimum source conductance.

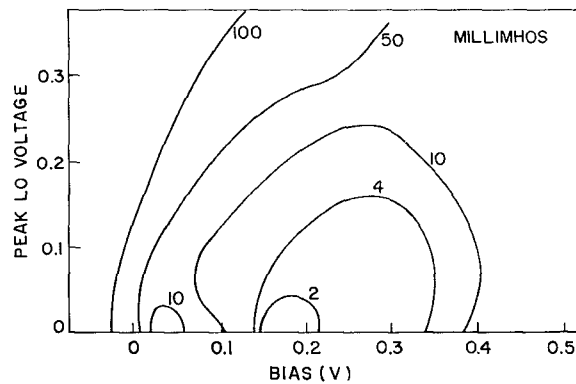


Fig. 9. GaSb diode optimum source conductance.

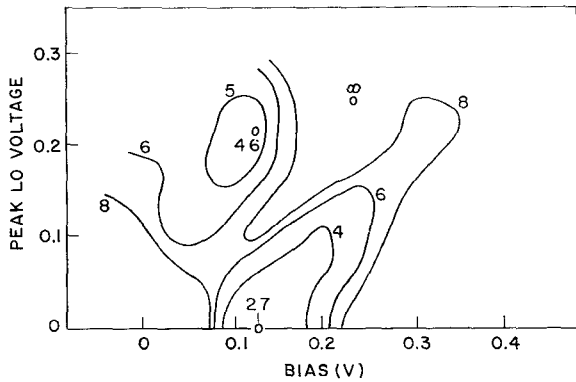


Fig. 10. Ge diode minimum noise factor.

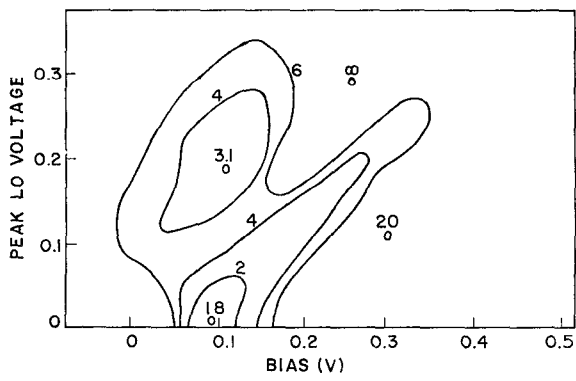


Fig. 11. GaSb diode minimum noise factor.

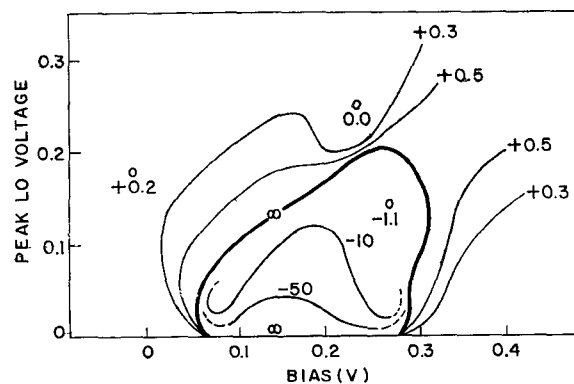


Fig. 12. Ge diode available gain.

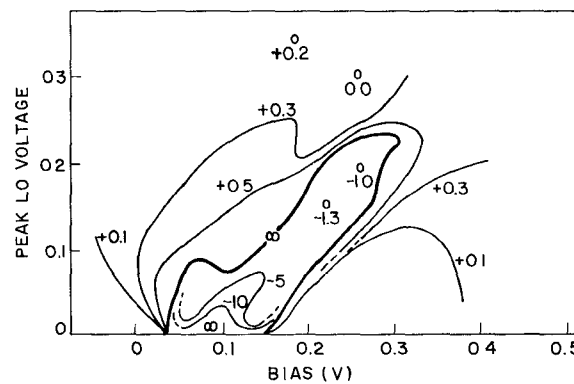


Fig. 13. GaSb diode available gain.

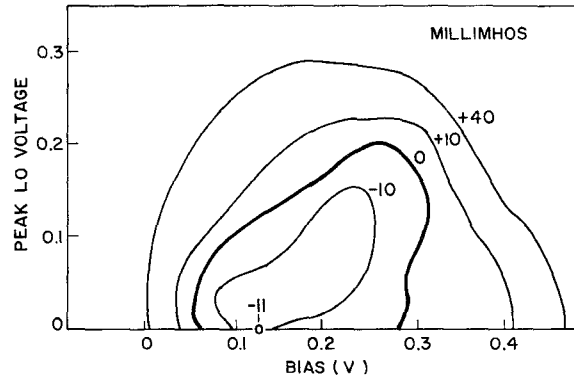


Fig. 14. Ge diode output conductance.

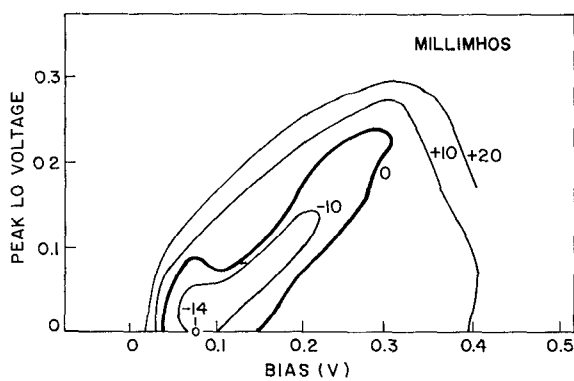


Fig. 15. GaSb diode output conductance.

DISCUSSION OF RESULTS

It is apparent from Figs. 10 and 11 that there are two modes of operation which yield reasonably low noise figures, both of these occur at a bias approximately equal to that which gives a minimum amplifier noise figure and they will be referred to as the large and small pump modes. It is coincidental that the large pump mode should have approximately the same bias point as the small pump mode since the modes are determined by different and unrelated considerations. Table I compares the essential features of the two modes:

TABLE I

	Mode	
	Large Pump	Small Pump
Available gain	~0.5	~ ∞
g_{out}	positive	negative
Noise figure ($g_{\gamma} = \infty$)	Ge 6.6 dB GaSb 4.9 dB	Ge 4.3 dB GaSb 2.5 dB

The large pump mode arouses the greatest practical interest because of its moderately low noise figure and noncritical adjustment. The available gain is comparable to the best conventional diode mixers, and the positive output conductance can easily be transformed to optimize the noise figure of an IF amplifier.

The small pump mode, on the other hand, is characterized by extremely critical adjustment of bias and source impedance. It is shown in the Appendix that the noise figure increases rapidly as the source conductance deviates from optimum, especially when the exchangeable gain becomes very large. It is also shown in the Appendix that the lowest noise figure obtainable with the small pump mode is equal to that using the tunnel diode as an amplifier and that the optimum bias voltage is the same in both cases. Although the exchangeable gain becomes very large with vanishing local-oscillator voltage, the output conductance is finite so that the overall noise figure of a tunnel diode and IF amplifier cascade approaches that of the mixer alone.

A surprising result is the negligibly small local oscillator power required to achieve the small pump mode; in practice -60 dBm has been used, which obviously implies a very poor dynamic range. The large pump mode, on the other hand, was found experimentally to have a dynamic range comparable to that obtained with conventional varistor mixers; for example, 1 dB compression at an input signal level of -6 dBm using a local oscillator power of -7 dBm.

A practical tunnel diode mixer-amplifier operating with a signal at 1350 Mc/s and 30 Mc/s IF has been tested using GaSb diodes having slopes of 20 and 60 ohms. The experimentally measured noise figures show

close agreement with the calculated values; for example, the 60-ohm diode in the large pump mode gave a minimum double sideband noise figure of 5.0 dB when connected to a source of 60 millimhos. These figures should be compared with those from Figs. 9 and 11 for the case of a short-circuited image, namely, 4.9 dB and 40 millimhos. The noise figure here applies to the mixer alone and was calculated from overall noise measurements on a mixer-preamplifier combination with and without a 3-dB pad separating the two units. The noise figure of the preamplifier with and without the pad had previously been determined as a function of source impedance.

When operated in the small pump mode a double-sideband noise figure of 4.3 dB was obtained at very high gain using a 60-ohm source. This should be compared with the 4.0 dB noise figure of the same diode used as an amplifier and the calculated value of 2.5 dB shown in Fig. 11 for a similar type of diode.

Observation of the voltage waveform across the nonlinear conductance using a 60-cycle generator of appropriate impedance showed it to be essentially sinusoidal. The amplitude was adjusted to give the same shift in bias voltage that is observed using the microwave local oscillator in the large pump mode. This evidence provides some confirmation of the sinusoidal assumption made throughout this paper but neglects the effects of junction capacitance and series inductance at higher frequencies.

CONCLUSIONS

The numerical analysis throws some light on the confusion which has existed in the literature concerning this subject. Two modes of low noise operation have been demonstrated one of which is suitable for a practical mixer, although the noise figure of a mixer-IF amplifier cascade using this large pump mode is 1 or 2 dB higher than that obtainable from a good L-band varistor mixer which is about 4 dB when the image is short-circuited. The dynamic range and pump power requirements are comparable to those of the conventional mixer and the positive output conductance can easily be transformed to drive a vacuum-tube amplifier.

The small pump mode, on the other hand, is only of academic interest because of its extremely critical adjustment procedure. The device in this mode is primarily a negative resistance amplifier with considerable gain and a noise figure of 3 or 4 dB. The noise performance is therefore comparable to the best varistor-diode mixers at L-band and is several dB better at higher frequencies. However, this small pump mode is impractical so that the minimum realistic noise figure of an ideal tunnel-diode mixer is essentially the same as that of any other good varistor, for example a point-contact down-converter.

If the high gain and low noise properties of the small

pump mode are required, it is better to use two diodes, the first as a negative resistance amplifier followed by a large pump mode down-converter or a varistor. In this way, the requirements are separated instead of combined and critical adjustment procedures are avoided.

It should be noted that the entire foregoing analysis required an optimized source conductance for every combination of bias and local oscillator voltage to give the lowest mixer noise figure. In practice it may be desirable to sacrifice mixer noise to achieve higher gain and thereby minimize an overall cascaded noise figure. The analysis techniques could also be applied to optimize backward diode converters [8] using megacycle intermediate frequencies. In these devices, only the large pump mode occurs, since there are no negative resistance effects. With kilocycle intermediate frequencies the $(1/f)$ noise would have to be included, however this noise is much lower in backward diodes than in conventional varistor mixers.

APPENDIX

MINIMUM NOISE FIGURE USING THE SMALL PUMP MODE

In the case of a vanishingly small local oscillator voltage, i.e., g_{e1} tending to zero, the optimum source conductance for low noise (12) has the binomial approximation:

$$g_{\alpha_{\text{opt}}} = |g_0| \left(1 + \frac{g_{e1}^2}{2g_0^2} - \frac{g_{e1}}{g_0} \frac{I_{e1}}{I_{e0}} \right). \quad (17)$$

If this value of $g_{\alpha_{\text{opt}}}$ is substituted in (11) and g_0 is assumed to be negative, the minimum noise figure becomes identical to that for the one-port tunnel-diode amplifier as g_{e1} approaches zero, i.e.,

$$F_{\text{min}} = 1 + \frac{e}{2kT} \cdot \frac{I_{e0}}{|g_0|}. \quad (18)$$

The noise figure (9) for an arbitrary source conductance may be written in the form:

$$F = F_{\text{min}} + \frac{eI_{e0}}{2kT} \cdot \frac{1}{|g_0|} \left(\frac{g_{\alpha} - g_{\alpha_{\text{opt}}}}{g_{e1}} \right)^2. \quad (19)$$

This shows that the noise figure increases rapidly as g_{α} deviates from the optimum value, especially when g_{e1} becomes very small at low levels of local oscillator voltage.

ACKNOWLEDGMENT

The author wishes to thank R. S. Engelbrecht and R. M. Ryder for many helpful comments and suggestions in connection with this project.

REFERENCES

- [1] K. K. N. Chang, G. H. Heilmeier, and H. J. Prager, "Low noise tunnel-diode down converter having conversion gain," *Proc. IRE*, vol. 48, pp. 854-858, May 1960.
- [2] D. I. Breitzer, "Noise figure of tunnel diode mixer," *Proc. IRE*, vol. 48, pp. 935-936, May 1960.
- [3] D. G. Peterson, "Tunnel diode down converters," *Proc. IRE*, vol. 49, pp. 1225-1226, July 1961.
- [4] Shih-Fang Lo, "Noise in tunnel diode mixers," *Proc. IRE*, vol. 49, pp. 1688-1689, November 1961.
- [5] R. A. Pucel, "Theory of the Esaki diode frequency converter," *Solid-State Electronics*, vol. 3, pp. 167-207, November 1961.
- [6] F. Sterzer, and A. Presser, "Stable low noise tunnel-diode frequency converters," *RCA Rev.*, vol. 23, pp. 3-28, March 1962.
- [7] L. E. Dickens and C. R. Gneiting, "A tunnel diode amplifying converter," *IRE Trans. on Microwave Theory and Techniques*, vol. MTT-9, pp. 99-101, January 1961.
- [8] C. A. Burrus, "Backward diodes for low-level millimeter-wave detection," *IEEE Trans. on Microwave Theory and Techniques*, vol. MTT-11, pp. 357-362, September 1963.
- [9] H. C. Torrey and C. A. Whitmer, *Crystal Rectifiers*, MIT Rad. Lab. Series no. 15, New York: McGraw-Hill, 1948.
- [10] H. A. Haus and R. B. Adler, "Extension of the noise figure definition," *Proc. IRE*, vol. 45, pp. 690-691, May 1957.
- [11] E. F. Bolinder, "Survey of some properties of linear networks," *IRE Trans. on Circuit Theory*, vol. CT-4, pp. 70-78, September 1957.
- [12] M. J. O. Strutt, "Noise figure reduction in mixer stages," *Proc. IRE*, vol. 34, pp. 942-950, December 1946.
- [13] R. A. Pucel, "Equivalent noise current of Esaki diodes," *Proc. IRE*, vol. 49, pp. 1080-1081, June 1961.
- [14] B. G. King and G. E. Sharpe, "Measurement of spot noise of Ge, GaSb, GaAs and Si Esaki diodes," *IEEE Trans. on Electron Devices*, vol. ED-11, pp. 273-285, June 1964.